The Coupling of Momentum Between Internal Gravity Waves and Mean Flow: A Numerical Study

WALTER L. JONES AND DAVID D. HOUGHTON[1]

National Center for Atmospheric Research,[2] Boulder, Colo.

(Manuscript received 16 November 1970, in revised form 15 February 1971)

ABSTRACT

A numerical model of internal gravity waves allows momentum transport by the waves to interact with the mean flow. Momentum deposited at a critical level develops a "shelf" in the mean flow. Mean flow acceleration Doppler-shifts the wave frequency, allowing more penetration of wave energy than expected from linear theory.

1. Introduction

Recently there has been considerable interest in the propagation of internal gravity waves in the vicinity of critical levels, levels at which the horizontal trace velocity of a wave equals the mean wind velocity. Approximate ray tracing theory, valid at large Richardson numbers (Bretherton, 1966), indicates that a wave packet approaches such a level asymptotically. More exact theory (Booker and Bretherton, 1967) shows that a small amount of wave energy is transmitted, but that at Richardson numbers >1–2 this flux is extremely small. Hazel (1967) demonstrated that the introduction of viscosity and conductivity causes dissipation of a wave close to the critical level without altering the reflection and transmission characteristics from the inviscid solution far from that level.

An internal gravity wave transports momentum. Eliassen and Palm (1961) have shown that the vertical flux of horizontal momentum of a steady-state internal gravity wave is constant, except at a critical level. Booker and Bretherton have shown that there is a discontinuity in the momentum flux at such a level. In the presence of dissipation this discontinuity becomes a steep gradient.

A discontinuity or gradient in the momentum flux implies an input of momentum to the mean flow and, consequently, a means of altering the mean flow. Lindzen and Holton (1968) have proposed such a mechanism as the cause of the quasi-biennial oscillation in the tropical upper atmosphere. In their model very low-frequency, tropically directed waves propagate upward, disposing of their momentum at a high-altitude critical level. The mean zonal wind is modified, the critical level moving downward with time. In the absence of other momentum transport mechanisms, a "shelf" is formed in the mean wind profile with its maximum at the critical velocity.

A numerical program has been developed for studying acoustic and internal gravity waves as transient phenomena in atmospheres with a mean flow (Houghton and Jones, 1969a, b). This program has been modified to include time variation of the mean wind as the result of gradients in the mean wave Reynolds stress. The time and space scales are quite different from those of Lindzen and Holton, but serve to illustrate the same effect. The model used does not realistically imitate some particular natural circumstances, but does provide qualitative conclusions. In particular, it shows that internal gravity waves of reasonable amplitude and scale can produce substantial changes in the mean wind in the upper stratosphere in a matter of hours. These changes are associated with transient wave behavior in an inviscid atmosphere. Additional details emerge from the model that were not deduced by Lindzen and Holton's parameterized approach; these details do not alter their basic conclusions, however.

2. The physical model

The geometry is planar and nonrotating, limiting the study to waves of periods up to a few hours and lengths up to a few thousand kilometers. The atmosphere is isothermal, compressible and inviscid up to 100 km; the speed of sound is 300 m sec^{-1}. Above 100 km a Rayleigh damping is gradually introduced, not to model physical phenomena, but to prevent reflection at the model top and to provide an effective radiation boundary condition. Motions are taken to be two-dimensional in the x and z directions.

The mean wind u_0 is taken to be in the x direction and to be a function of z. Initially, it increases uniformly from zero at the ground to 100 m sec^{-1} at 100 km. In

[1] Present affiliation: Department of Meteorology, University of Wisconsin, Madison.
[2] The National Center for Atmospheric Research is sponsored by the National Science Foundation.

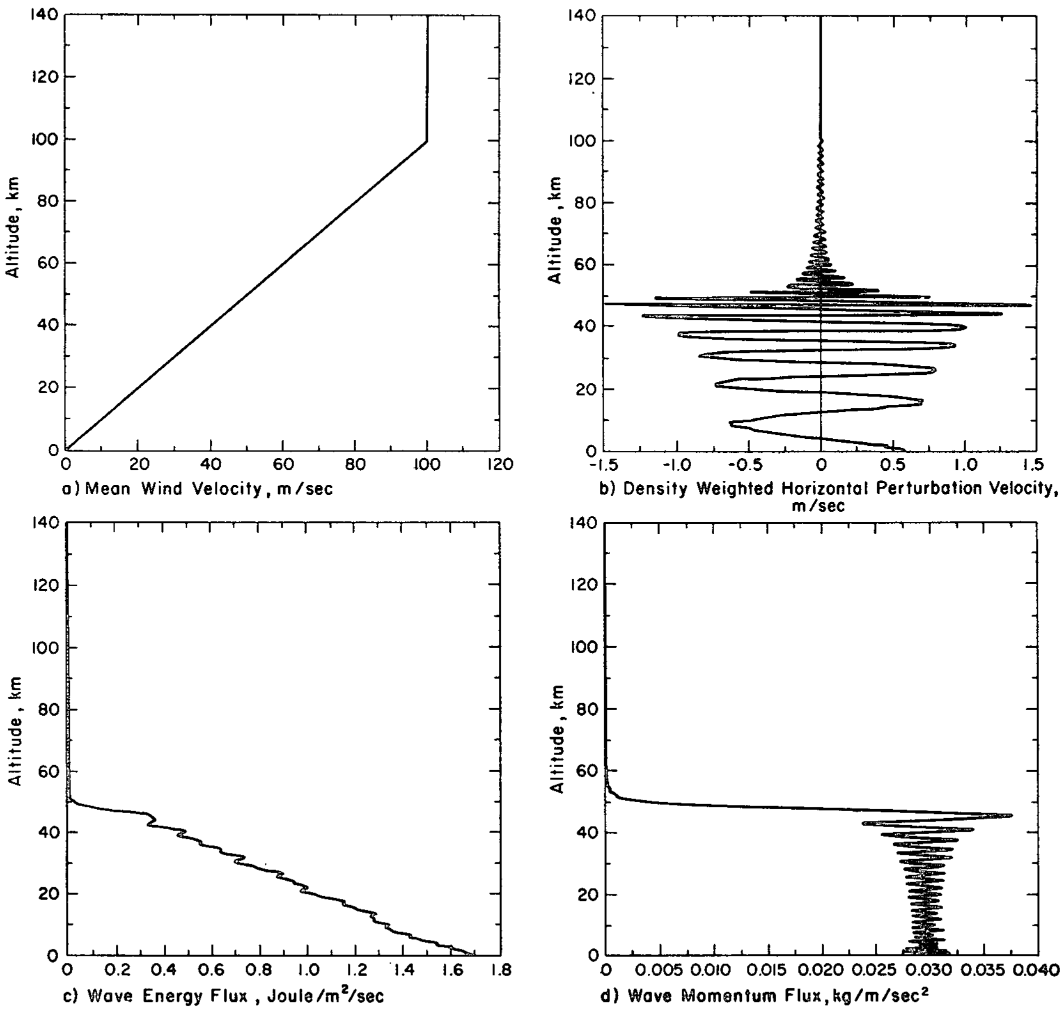

Fig. 1. Characteristic properties of mean flow and an internal gravity wave as functions of altitude 12 hr after start, with no momentum coupling between mean flow and waves: a) mean flow; b) product of perturbation flow amplitude and square root of mean density [$\rho_0(0)=1.225$ kg m^{-3}]; c) vertical flux of wave energy, $\overline{p_1 w_1}$; d) Reynolds stress component, $\rho_0\overline{u_1 w_1}$.

this study u_0 is allowed to vary with time in response to the mean value of the vertical gradient of the wave momentum flux, $\rho_0\overline{u_1 w_1}$, where subscript 0 refers to the mean state, subscript 1 to the linear perturbation, and an overbar denotes an average over a horizontal wavelength.

The wave is generated at the bottom boundary; in effect, a sinusoidally corrugated boundary is accelerated up to a fixed velocity in the x direction, starting at time $t=0$. The wavelength of the corrugation is 100 km, and the wave period 0.5 hr relative to an observer on the ground. The wave trace velocity is thus 56 m sec^{-1} and initially there is a critical level at 56 km. The standard linearized equations of motion and mass continuity and the adiabatic thermal equation for a perfect gas are used to compute the wave perturbations. The amplitude of the vertical velocity perturbation was taken to be 10 cm sec^{-1} at the ground.

3. The numerical model

The essentials of the numerical scheme are given in Houghton and Jones (1969a, b) and will not be repeated in detail here. Basically, all derivatives are centered with exceptions as noted below and the grid points are staggered in space and time. The equations for computing time derivatives of the field variables are the same as shown in Houghton and Jones with the addition of a term containing the factor $\rho_1(\partial u_0/\partial t)$ to the horizontal equation of motion. The equation

$$\frac{\partial u_0}{\partial t}=-\frac{1}{2\rho_0}\frac{\partial}{\partial z}[\mathrm{Re}(\rho_0 u_1 w_1^*)]$$

is used to compute time changes in the mean velocity, where w_1^* is the complex conjugate of w_1.

The variable $\mathrm{Re}(\rho_0 u_1 w_1^*)$ was computed at the grid points where u_1, ρ_1 and p_1 were defined. Then $\partial u_0/\partial t$

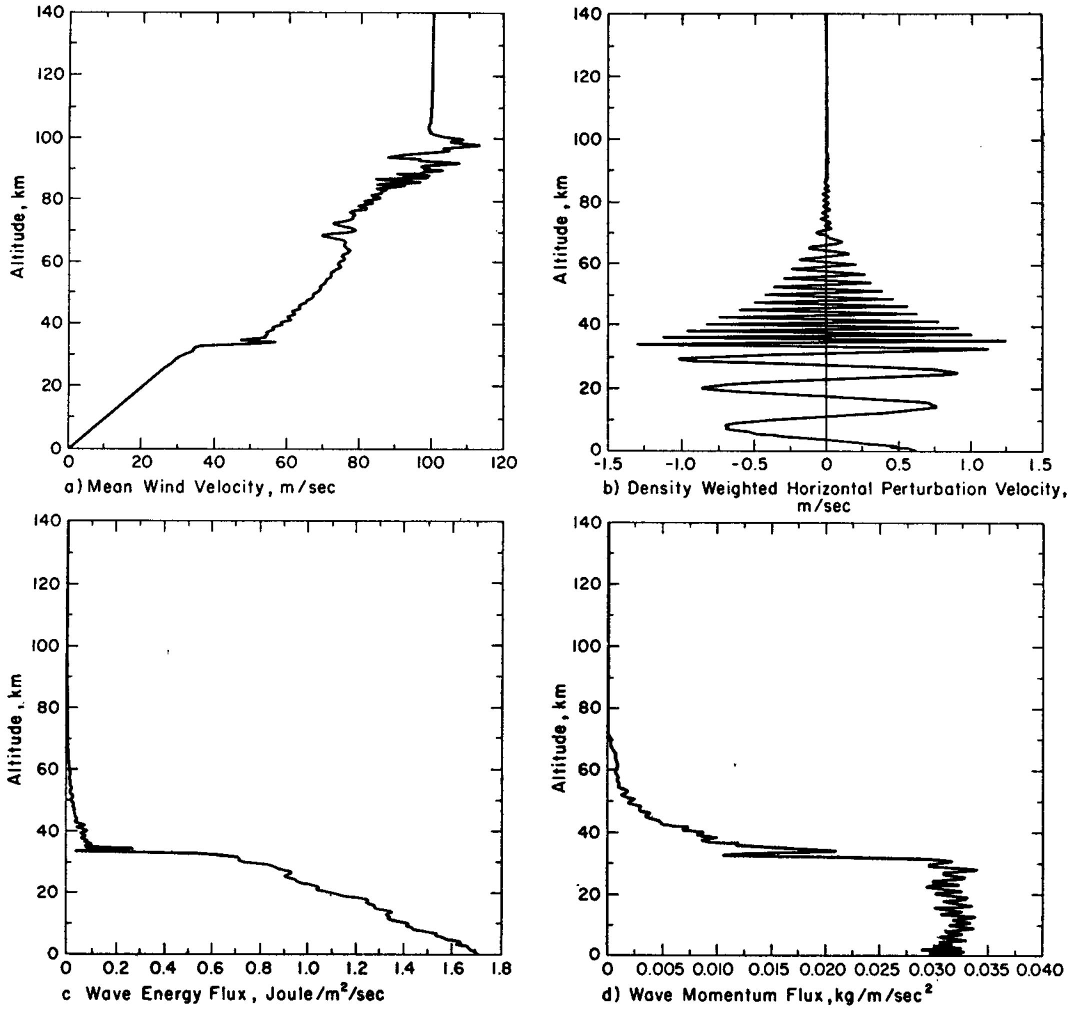

FIG. 2. Characteristic properties of mean flow and an internal gravity wave as functions of height 12 hours after start, with momentum coupling between mean flow and waves. Graphs correspond to those of Fig. 1.

was computed at the grid levels of w_1, but intermediate in time. This placed u_0 at the grid points of w_1 and permitted the direct computation of $\partial u_0/\partial z$ at the u_1, ρ_1 and p_1 grid levels, but at the midpoint in time exactly where it was needed for the horizontal equation of motion.

The mean velocity variables were advanced to the next time step after the perturbation variables were advanced. Since the model had fine resolution in time (a $\frac{3}{4}$-sec time increment was used), the magnitude of u_0 was updated only once every 10 time steps wherever it appeared undifferentiated in the prediction equations. However, where u_0 appeared in differentiated form in the horizontal equation of motion, it was updated every time step. The ρ_1 in the calculation of the $\rho_1(\partial u_0/\partial t)$ term was centered in time although $\partial u_0/\partial t$ itself was not. This was handled by making a preliminary computation to obtain a new value of ρ_1 using a forward-difference form in the ρ_1 prediction equation. No numerical difficulties were found to result from the less rigorous treatment of the $\rho_1(\partial u_0/\partial t)$ term.

Boundary conditions to close the finite-difference equations had to be prescribed. At the lower boundary the vertical stress gradient was taken to be zero, making $\partial u_0/\partial t=0$ and u_0 a constant in time consistent with a Prandtl layer formulation. At the upper boundary the vertical stress gradient was taken to be constant so that $\partial u_0/\partial t$ was the same at the upper boundary as it was one grid point below. Since u_0 was initially the same at these two points, it remained the same for all time.

The variable ρ_0 in the prediction equation for $\partial u_0/\partial t$ makes the mean velocity very sensitive to any wave disturbances in the model above 100 km. In order to control the solution above 100 km, a Rayleigh damping was applied to oscillations of the mean velocity in the same way as it was applied to the velocity associated with the wave motions. The mean velocity was relaxed to an equilibrium value of 100 m sec^{-1}, whereas the perturbation velocities were relaxed to a zero value. The same damping coefficient was used for both relaxations. The coefficients varied approximately exponentially with height starting from zero at 100 km and increasing to a magnitude at the upper boundary which produced a 5% reduction in the difference between the velocity magnitude and its equilibrium state every time step.

4. Results

Two runs were made for comparative purposes. The first had no momentum coupling to the mean flow and is a conventional linear analysis. The state after 12 hr is shown in Fig. 1. The horizontal wind in Fig. 1b is weighted with $\rho_0^{\frac{1}{2}}$ in order to balance out the exponential growth of propagating gravity waves. Stemming from density variation, $u_1\rho_0^{\frac{1}{2}}$ is a field variable (Eckart, 1960). In a steady state the envelope of $u_1\rho_0^{\frac{1}{2}}$ should vary as $(z_0-z)^{-\frac{1}{2}}$ below the critical level at z_0. This behavior has begun to build up after 12 hr.

There is some wave activity above 56 km. It is not, however, the predicted steady-state wave leakage, which is much smaller. Instead, the start-up process has introduced transient wave energy over a range of frequencies. The higher frequency components approach a range of critical levels at greater heights. The time for a wave packet to reach a given distance from its critical level is proportionately less dependent on initial conditions for long times; hence, most of these "wave packets" are at about the same distance from their critical levels and have similar vertical scales.

Fig. 1c shows the vertical flux of wave energy, $\overline{p_1w_1}$. In the steady state this should decrease linearly to zero at the critical level and remain negligible at higher levels. The momentum flux is shown in Fig. 1d. In the steady state this should be constant up to a discontinuity at the critical level. Both figures show transient oscillations that decrease with time and average to zero over several wave periods. The gradient of momentum flux lies below the critical level and steepens with time.

The second run was made with momentum coupling to the mean flow; the effects of this coupling being evident in Fig. 2a. A shelf has formed in the wind profile. The temporal development of this shelf is shown in Fig. 3. After 4 hr the wave has just begun to approach the critical level and the momentum flux gradient is rather shallow as the gradient steepens in time. The mean flow acceleration increases with time and is concentrated at the lower edge of the shelf.

The parameterized Lindzen-Holton model allows no wave leakage past the critical level. Therefore, its mean wind profile is uniform above the shelf at a velocity equal to the trace velocity of the wave. In our result there is some mean flow acceleration to velocities greater than the trace velocity. Also, there is considerable wave activity above the critical level as evidenced by Figs. 2b–d. Apparently, there is more leakage of energy in the coupled system.

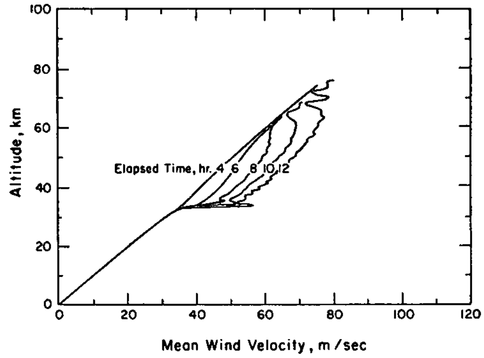

FIG. 3. Mean flow profile at several different elapsed times for model with momentum coupling.

We attribute most of this leakage to the fact that the wave is passing through a region of accelerating mean flow. Within the geometrical optics approximation (Jones, 1969) it can be shown that a local acceleration in the mean flow causes a shift in the frequency of a wave packet relative to a fixed reference frame. This, in turn, causes a shift in the trace velocity of the wave. In this problem the acceleration of the trace velocity is equal to that of the mean flow. Wave energy in the accelerating shelf will then have a trace velocity >56 m sec^{-1}. The more widely separated the time scales of wave and mean flows, the less important this acceleration effect will be.

Unfortunately, it is difficult to predict the exact results under the WKB approximation and hence sort out non-WKB effects. A packet in a uniformly accelerated fluid will at any time see the same change in its horizontal trace velocity as the change in mean velocity. On the other hand, consider this crude process: a packet is accelerated in one volume, propagates upward to an as-yet-unaccelerated volume which is then accelerated, and so on. The total change in the packet's trace velocity will exceed the total change in the mean velocity of the volume it occupies. Nevertheless, wave packets arriving after the mean flow has changed partially will experience smaller Doppler shifts.

At 12 hr the mean flow over 40–60 km has changed by $\sim$18 m sec^{-1} and at least some of the wave energy may be associated with trace velocities with larger changes. (A reviewer has pointed out that the vertical wave scale at 60 km implies changes of trace velocity of 28 m sec^{-1}.)

A considerable amount of oscillation in the mean flow appears a little below 100 km. (Above this height Rayleigh damping suppresses such motion.) Small transient wave disturbances reaching this height produce strong effects, since the mean density is very low. As time passes, more and more such disturbances reach this level and at 14–16 hr the oscillations in the mean flow are out of hand. The increased amount of wave energy reaching these levels probably reflects the effects of shelf acceleration, although the drastically decreased Richardson number at the shelf bottom may also play a role. We attach little physical significance to these oscillations.

Gravity waves can establish and presumably maintain a sharp gradient of the mean flow in the presence of momentum diffusion processes (Lindzen, 1968; Gossard *et al.*, 1970). Such sharp gradients might be related to the creation of clear air turbulence. They might be formed in a period of hours by waves whose ground-level amplitudes are within existing synoptic meteorological noise levels.

REFERENCES

Booker, J. R., and F. P. Bretherton, 1967: The critical layer for internal gravity waves in a shear flow. *J. Fluid Mech.*, **27**, 513–539.

Bretherton, F. P., 1966: The propagation of groups of internal gravity waves in a shear flow. *Quart. J. Roy. Meteor. Soc.*, **92**, 466–480.

Eckart, C. H., 1960: *Hydrodynamics of Oceans and Atmospheres.* New York, Pergamon Press, 290 pp.

Eliassen, A., and E. Palm, 1961: On the transfer of energy in stationary mountain waves. *Geofys. Publikasjoner*, **22**, No. 3, 1–23.

Gossard, E. E., J. H. Richter and D. Atlas, 1970: Internal waves in the atmosphere from high resolution radar measurements. *J. Geophys. Res.*, **75**, 3523–3536. (See also Comments by C. O. Hines, **75**, 5956–5959.)

Hazel, P., 1967: The effect of viscosity and heat conduction on internal gravity waves at a critical level. *J. Fluid Mech.*, **30**, 775–783.

Houghton, D. D., and W. L. Jones, 1969a: A numerical model for linearized gravity and acoustic waves. *J. Comput. Phys.*, **3**, 339–357.

——, and ——, 1969b: Gravity wave propagation with a time-dependent critical level. *Proc. Symp. Acoustic-Gravity Waves in the Atmosphere*, Boulder, Colo., Government Printing Office, p. 241.

Jones, W. L., 1969: Ray tracing for internal gravity waves. *J. Geophys. Res.*, **74**, 2028–2033.

Lindzen, R. S., 1968: Some speculations on the roles of critical level interactions between internal gravity waves and mean flows. *Proc. Symp. Acoustic-Gravity Waves in the Atmosphere*, Boulder, Colo., Government Printing Office.

——, and J. R. Holton, 1968: A theory of the quasi-biennial oscillation. *J. Atmos. Sci.*, **25**, 1095–1107.